BRAIDS, METALLIC RATIOS AND PERIODIC SOLUTIONS OF THE $2n$-BODY PROBLEM

YUIKA KAJIHARA, EIKO KIN, AND MITSURU SHIBAYAMA

ABSTRACT. Periodic solutions of the planar N-body problem determine braids through the trajectory of N bodies. Braid types can be used to classify periodic solutions. According to the Nielsen-Thurston classification of surface automorphisms, braids fall into three types: periodic, reducible and pseudo-Anosov. To a braid of pseudo-Anosov type, there is an associated stretch factor greater than 1, and this is a conjugacy invariant of braids. In 2006, the third author discovered a family of multiple choreographic solutions of the planar $2n$-body problem. We prove that braids obtained from the solutions in the family are of pseudo-Anosov type, and their stretch factors are expressed in metallic ratios. New numerical periodic solutions of the planar $2n$-body problem are also provided.

1. INTRODUCTION

Consider the motion of m points in the plane $\mathbb{R}^2$

$$\boldsymbol{x}(t) = (x_1(t), \dots, x_m(t)),$$

where $x_i(t) \in \mathbb{R}^2$ is the position of the ith point at $t \in \mathbb{R}$. Let $Q_m(t) = \{x_1(t), \dots, x_m(t)\}$. We assume the following.

- $\boldsymbol{x}(t)$ is collision-free, i.e., for any $t \in \mathbb{R}$, $x_i(t) \neq x_j(t)$ if $i \neq j$.
- There exists $t_0 > 0$ such that

$$Q_m(t + t_0) = Q_m(t).$$

Then we have a (geometric) braid

$$b(\boldsymbol{x}(t), [0, t_0]) = \bigcup_{t \in [0, t_0]} \big\{(x_1(t), t), \dots, (x_m(t), t)\big\} \subset \mathbb{R}^2 \times [0, t_0]$$

with base points $Q_m(0)(= Q_m(t_0))$. The actual location of base points is irrelevant for the study of braids. To remove the data of the location, we

Date: July 6, 2023 .

2020 *Mathematics Subject Classification.* 57K10, 57K20, 70F10.

Key words and phrases. N-body problem, periodic solutions, braid groups, pseudo-Anosov braids, metallic ratio, stretch factor.

Y. K. was supported by JSPS KAKENHI Grant Number JP20J21214.
E. K. was supported by JSPS KAKENHI Grant Number JP18K03299 and JP21K03247.
M. S. was supported by JSPS KAKENHI Grant Number JP18K03366.

.

consider its *braid type* $\langle b(\boldsymbol{x}(t), [0, t_0]) \rangle$ instead of the braid. A braid type $\langle b \rangle$ of a braid b is *not* an element of the braid group. It is the conjugacy class of the projection of b in the projective braid group. (See Definition 3.2 for the definition of braid types.)

We investigate periodic solutions of the planar N-body problem given by the following ODEs.

$$m_i \ddot{x}_i = -\sum_{j \neq i} m_i m_j \frac{x_i - x_j}{|x_i - x_j|^3}, \quad x_i \in \mathbb{R}^2,\ m_i > 0\ (i = 1, \dots, N). \tag{1.1}$$

Suppose that $\boldsymbol{x}(t) = (x_1(t), \dots, x_N(t))$ is a periodic solution with period T of (1.1). The solution $\boldsymbol{x}(t)$ determines a (pure) braid $b(\boldsymbol{x}(t), [0, T])$ and its braid type $\langle b(\boldsymbol{x}(t), [0, T] \rangle$. For the definition of pure braids, see Definition 3.1. Braid types can be used to classify periodic solutions of the planar N-body problem.

Question 1.1 (Montgomery [Mona, Monb], (cf. Moore [Moo93]))**.** *For any pure braid b with N strands, is there a periodic solution of the planar N-body problem whose braid type is equal to $\langle b \rangle$?*

Question 1.1 is wide open for every $N > 3$. For example we do not even know of a single braid type which is *not* realized when $N = 4$. In the case of $N = 3$ and non-zero, yet small angular momentum, Question 1.1 is true by work of Moeckel-Montgomery [MM15]. For other studies on braids obtained from periodic solutions, see a pioneer work by Moore [Moo93]. See also [FGA21, MS13, Mon98, Monb].

Remark 1.2. *We consider the following Newton equations*

$$m_i \ddot{x}_i = -\sum_{j \neq i} m_i m_j \frac{x_i - x_j}{|x_i - x_j|^{\alpha+1}}, \quad x_i \in \mathbb{R}^2,\ m_i > 0\ (i = 1, \dots, N), \tag{1.2}$$

where $\alpha \geq 1$. The case $\alpha = 2$ corresponds to (1.1) describing the motion of n bodies under the influence of gravitation. One can ask the same question as Question 1.1 for the planar N-body problem given by (1.2). It is known by Montgomery [Mon98] *that Question 1.1 is true for any "tied" braid type when $\alpha \geq 3$ (i.e., under the assumption that the force is strong).*

According to the Nielsen-Thurston classification of surface automorphisms [FLP79], braids fall into three types: periodic, reducible and pseudo-Anosov. (See Section 3.3.) To a braid b of pseudo-Anosov type, there is an associated stretch factor $\lambda(b) > 1$, and this is a conjugacy invariant of pseudo-Anosov braids. Since the Nielsen-Thurston type is also a conjugacy invariant, one can define the stretch factor $\lambda(\langle b \rangle) := \lambda(b)$ for the pseudo-Anosov braid type $\langle b \rangle$ of b. See (3.1) in Section 3.3.

The stretch factor tells us a dynamical complexity of pseudo-Anosov braids. In this paper we ask the following question related to Question 1.1.

Question 1.3. *Let b be a pure braid with N strands. Suppose that b is of pseudo-Anosov type. Is there a periodic solution of the planar N-body problem whose braid type is equal to $\langle b \rangle$?*

The stretch factor of each pseudo-Anosov braid with 3 strands is a quadratic irrational (Section 3.4). This is not necessarily true for pseudo-Anosov braids with more than 3 strands. Moore [Moo93] and Chenciner-Montgomery [CM00] found a simple choreographic solution to the 3-body problem such that the three bodies chase one another along a figure-8 curve. The braid type of the solution is pseudo-Anosov and its stretch factor is the 6th power of the 1st metallic ratio $\mathfrak{s}_1$ (Example 3.8), i.e., golden ratio, where the kth metallic ratio $\mathfrak{s}_k$ ($k \in \mathbb{N}$) is given by

$$\mathfrak{s}_k = \frac{1}{2}(k + \sqrt{k^2+4}) = k + \cfrac{1}{k + \cfrac{1}{k + \cfrac{1}{k + \ddots}}}$$

The study of braid types of the periodic solutions has been relatively less investigated. We hope that the following result sheds some light on Question 1.3. Let $\lfloor \cdot \rfloor$ be the floor function.

Theorem 1.4. *For $n \geq 2$ and $p \in \{1, \ldots, \lfloor \frac{n}{2} \rfloor\}$, there exists a zero angular momentum periodic solution $\boldsymbol{x}_{n,p}(t)$ of the planar $2n$-body problem with equal masses whose braid type $X_{n,p}$ is pseudo-Anosov with the stretch factor $(\mathfrak{s}_{2p})^{\frac{2n}{d}}$, where $d = \gcd(n,p)$.*

A representative of the braid type $X_{n,p}$ in Theorem 1.4 is the $(\frac{n}{d})$th power $(\beta_{n,p})^{\frac{n}{d}}$ of the $2n$-braid $\beta_{n,p}$ introduced in Section 4. In 2006, the third author proved the existence of a family of multiple choreographic solutions

$$\boldsymbol{x}_{n,p}(t) = (x_1(t), \ldots, x_{2n}(t))$$

of the planer $2n$-body problem with equal masses [Shi06]. Some of the solutions in the family had already been found by Chen [Che01, Che03] and Ferraio-Terracini [FT04]. The orbit of the periodic solution $\boldsymbol{x}_{n,p}(t)$ consists of $2d$ closed curves, each of which is the trajectory of $\frac{n}{d}$ bodies. The braid types $X_{n,p}(t)$ in Theorem 1.4 are realized by $\boldsymbol{x}_{n,p}(t)$ given in [Shi06]. More precisely, it is proved in [Shi06] that for $n \geq 2$ and $p \in \{1, \ldots, \lfloor \frac{n}{2} \rfloor\}$, there exists a zero angular momentum periodic solution $\boldsymbol{x}_{n,p}(t)$ with period $T > 0$ of the planar $2n$-body problem such that

$$x_i(t + (\tfrac{d}{n})T) = x_{\sigma_{n,p}(i)}(t) \ \text{ for } \ i = 1, \ldots, 2n,$$

where $\sigma_{n,p} = (1, 3, \ldots, 2n-1)^p (2, 4, \ldots, 2n)^{-p} \in \mathfrak{S}_{2n}$ is a permutation of $2n$ elements. Thus, the (non-pure) braid $y_{n,p} := b(\boldsymbol{x}_{n,p}(t), [0, (\frac{d}{n})T])$ and the corresponding braid type $Y_{n,p} := \langle y_{n,p} \rangle$ are obtained from the solution $\boldsymbol{x}_{n,p}(t)$, and the $(\frac{n}{d})$th power $(y_{n,p})^{\frac{n}{d}}$ (which is a pure braid) represents the

braid type $X_{n,p}$. See Figure 1 for periodic solutions $\boldsymbol{x}_{n,p}(t)$ for $0 \leq t \leq (\frac{d}{n})T$. Theorem 1.4 follows from the following (see Remark 3.6).

Theorem 1.5. *For $n \geq 2$ and $p \in \{1, \ldots, \lfloor \frac{n}{2} \rfloor\}$, the braid type $Y_{n,p}$ is pseudo-Anosov with the stretch factor $(\mathfrak{s}_{2p})^2$. In particular, the braid type $X_{n,p}$ of the solution $\boldsymbol{x}_{n,p}(t)$ is pseudo-Anosov with the stretch factor $(\mathfrak{s}_{2p})^{\frac{2n}{d}}$.*

Since $\mathfrak{s}_k < \mathfrak{s}_{k'}$ if $k < k'$, we immediately have the following result.

Corollary 1.6. *Let $X_{n,p}$ be the braid type as in Theorem 1.5. For $n \geq 2$ and $p, p' \in \{1, \ldots, \lfloor \frac{n}{2} \rfloor\}$ with $p < p'$, we have the following.*

1. *$\lambda(X_{n,p}) < \lambda(X_{n,p'})$ if $\gcd(n,p) = \gcd(n,p')$. In particular $X_{n,p} \neq X_{n,p'}$.*
2. *$\lambda(X_{n,p}) < \lambda(X_{n,p'})$ if n is prime. In particular $X_{n,p} \neq X_{n,p'}$.*

The $2n$ bodies for the solution $\boldsymbol{x}_{n,p}(t)$ form a regular $2n$-gon at the initial time $t = 0$, and the next first time is $t = (\frac{d}{2n})T$ when the $2n$ bodies form a regular $2n$-gon again. See Figure 1 for $\boldsymbol{x}_{n,p}(t)$ at $t = (\frac{d}{2n})T$. From the viewpoint of the configuration of the "next" regular $2n$-gon, it is proved in [Shi06] that $\boldsymbol{x}_{n,p}(t)$ and $\boldsymbol{x}_{n,p'}(t)$ are distinct solutions for distinct $p, p' \in \{1, \ldots, \lfloor \frac{n}{2} \rfloor\}$ (Remark 2.1). On the other hand, from the viewpoint of braid

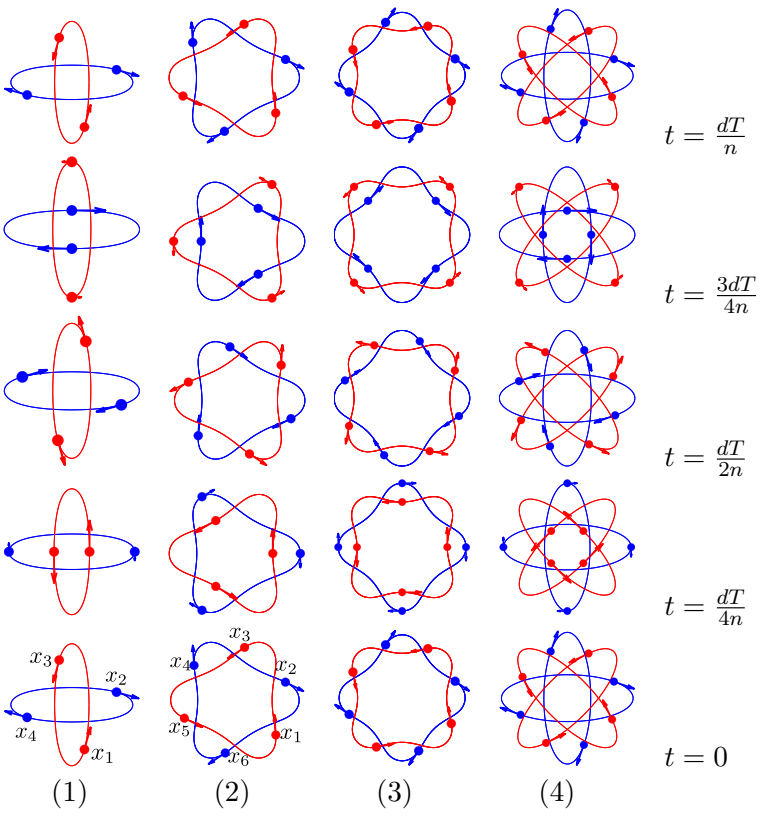

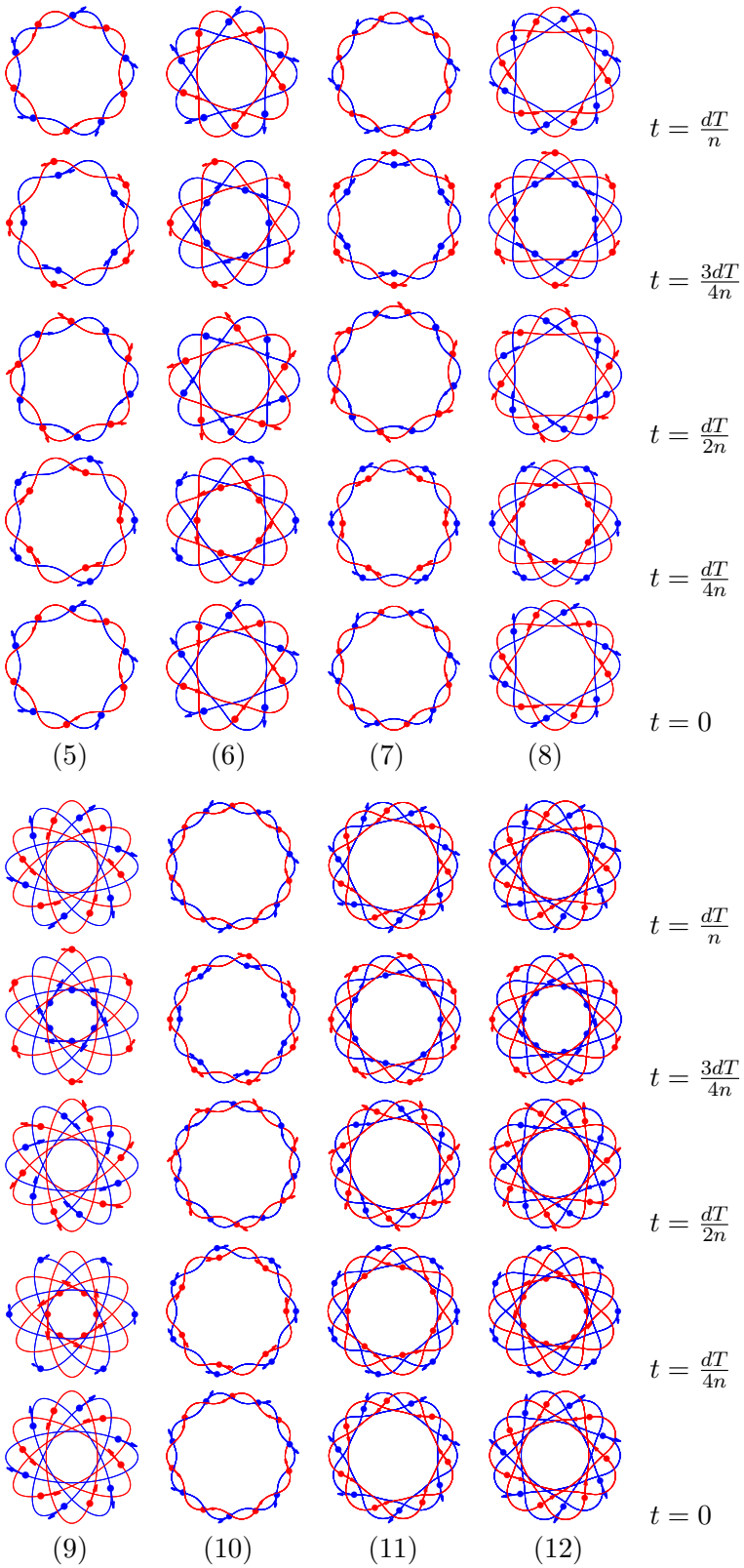

Figure 1. $\boldsymbol{x}_{n,p}(t)$ for $0 \le t \le (\frac{d}{n})T$: (1) $\boldsymbol{x}_{2,1}(t)$. (2) $\boldsymbol{x}_{3,1}(t)$. (3) $\boldsymbol{x}_{4,1}(t)$. (4) $\boldsymbol{x}_{4,2}(t)$. (5) $\boldsymbol{x}_{5,1}(t)$. (6) $\boldsymbol{x}_{5,2}(t)$. (7) $\boldsymbol{x}_{6,1}(t)$. (8) $\boldsymbol{x}_{6,2}(t)$. (9) $\boldsymbol{x}_{6,3}(t)$. (10) $\boldsymbol{x}_{7,1}(t)$. (11) $\boldsymbol{x}_{7,2}(t)$. (12) $\boldsymbol{x}_{7,3}(t)$.

types, Corollary 1.6 tells us that $X_{n,p}$ is different from $X_{n,p'}$ if $\gcd(n,p) = \gcd(n,p')$.

Table 1 shows the stretch factor $\lambda_{n,p} = \lambda(X_{n,p})$ and the entropy $\log(\lambda_{n,p})$ for several pairs (n,p). One can see from this table that $\lambda(X_{n,p}) \neq \lambda(X_{n,p'})$ if $p \neq p'$ up to $n = 11$. Therefore the braid types $X_{n,p}$ and $X_{n,p'}$ of the solutions for $p \neq p' \in \{1, \ldots, \lfloor \frac{n}{2} \rfloor\}$ are distinct up to $n = 11$.

Because of an intriguing formula of metallic ratios, $\mathfrak{s}_k^3 = \mathfrak{s}_{k^3+3k}$ for example, stretch factors $\lambda(X_{n,p})$ happen to coincide with the ones for different pairs (n,p') occasionally (see Example 4.1). Nevertheless, we conjecture that $X_{n,p} \neq X_{n,p'}$ for all $p, p' \in \{1, \ldots, \lfloor \frac{n}{2} \rfloor\}$ with $p \neq p'$.

The organization of the paper is as follows. In Section 2 we introduce a family of periodic solutions $\boldsymbol{x}_{n,p}(t)$ in [Shi06] of the planar $2n$-body problem and describe the symmetries of the solutions. In Section 3 we briefly review the necessary background on braid groups. We prove Theorem 1.5 in Section 4. In Section 5, we give new numerical periodic solutions $\boldsymbol{x}_{n,p}(t)$ of the planar $2n$-body problem when $p > \lfloor \frac{n}{2} \rfloor$.

2. Periodic solutions of the planar $2n$-body problem

This section is devoted to explaining the periodic solutions $\boldsymbol{x}_{n,p}(t)$. The existence was proven with the variational method. They have high symmetries because they can be represented as elements of a functional space limited by several group actions. The minimizers of the action functional under the symmetry correspond to those solutions. They are also regarded as orbits on the *shape sphere*. They are constructed through minimizing methods, and we omit analytic techniques for the proof and describe geometric properties of $\boldsymbol{x}_{n,p}(t)$ including the group actions and shape sphere.

2.1. **Symmetry.**

Let G be a finite group. We consider a 2-dimensional orthogonal representation $\rho : G \to O(2)$, a homomorphism $\sigma : G \to \mathfrak{S}_{2n}$ to the symmetric group on $2n$ elements, and another 2-dimensional orthogonal representation $\tau : G \to O(2)$. We will denote by Λ, the set of T-periodic orbits. The action of G to Λ is defined by

$$g \cdot ((x_1, \ldots, x_{2n})(t)) = (\rho(g)x_{\sigma(g^{-1})(1)}, \ldots, \rho(g)x_{\sigma(g^{-1})(2n)})(\tau(g^{-1})(t))$$

for $g \in G$ and $\boldsymbol{x}(t) = (x_1, \ldots, x_{2n})(t) \in \Lambda$, where the above ρ, σ, τ represent respectively actions of G on $\mathbb{R}^2$ by orthogonal transformations, on indices $\{1, 2, \ldots, 2n\}$ by permutations, and on the circle $\mathbb{R}/T\mathbb{Z}$. Specifically, we take G as the group $G_{n,p} := \langle g_n, h_{n,p} \rangle$ generated by the two elements g_n and

Table 1. Some examples obtained from Theorem 1.4.

(n,p)	d	$X_{n,p}=\langle(\beta_{n,p})^{\frac{n}{d}}\rangle$	$\lambda_{n,p}=(\mathfrak{s}_{2p})^{\frac{2n}{d}}$	$\log(\lambda_{n,p})=(\frac{2n}{d})\log(\mathfrak{s}_{2,p})$
$(2,1)$	1	$(\beta_{2,1})^2$	$(\mathfrak{s}_2)^4$	3.525494348078172
$(3,1)$	1	$(\beta_{3,1})^3$	$(\mathfrak{s}_2)^6$	5.288241522117257
$(4,1)$	1	$(\beta_{4,1})^4$	$(\mathfrak{s}_2)^8$	7.050988696156343
$(4,2)$	2	$(\beta_{4,2})^2$	$(\mathfrak{s}_4)^4$	5.774541900715241
$(5,1)$	1	$(\beta_{5,1})^5$	$(\mathfrak{s}_2)^{10}$	8.813735870195430
$(5,2)$	1	$(\beta_{5,2})^5$	$(\mathfrak{s}_4)^{10}$	14.436354751788103
$(6,1)$	1	$(\beta_{6,1})^6$	$(\mathfrak{s}_2)^{12}$	10.576483044234514
$(6,2)$	2	$(\beta_{6,2})^3$	$(\mathfrak{s}_4)^6$	8.661812851072861
$(6,3)$	3	$(\beta_{6,3})^2$	$(\mathfrak{s}_6)^4$	7.273785836928267
$(7,1)$	1	$(\beta_{7,1})^7$	$(\mathfrak{s}_2)^{14}$	12.339230218273601
$(7,2)$	1	$(\beta_{7,2})^7$	$(\mathfrak{s}_4)^{14}$	20.210896652503344
$(7,3)$	1	$(\beta_{7,3})^7$	$(\mathfrak{s}_6)^{14}$	25.458250429248935
$(8,1)$	1	$(\beta_{8,1})^8$	$(\mathfrak{s}_2)^{16}$	14.101977392312687
$(8,2)$	2	$(\beta_{8,2})^4$	$(\mathfrak{s}_4)^8$	11.549083801430482
$(8,3)$	1	$(\beta_{8,3})^8$	$(\mathfrak{s}_6)^{16}$	29.095143347713069
$(8,4)$	4	$(\beta_{8,4})^2$	$(\mathfrak{s}_8)^4$	8.378850189044405
$(9,1)$	1	$(\beta_{9,1})^9$	$(\mathfrak{s}_2)^{18}$	15.864724566351773
$(9,2)$	1	$(\beta_{9,2})^9$	$(\mathfrak{s}_4)^{18}$	25.985438553218586
$(9,3)$	3	$(\beta_{9,3})^3$	$(\mathfrak{s}_6)^6$	10.910678755392400
$(9,4)$	1	$(\beta_{9,4})^9$	$(\mathfrak{s}_8)^{18}$	37.704825850699820
$(10,1)$	1	$(\beta_{10,1})^{10}$	$(\mathfrak{s}_2)^{20}$	17.627471740390860
$(10,2)$	2	$(\beta_{10,2})^5$	$(\mathfrak{s}_4)^{10}$	14.436354751788103
$(10,3)$	1	$(\beta_{10,3})^{10}$	$(\mathfrak{s}_6)^{20}$	36.368929184641338
$(10,4)$	2	$(\beta_{10,4})^5$	$(\mathfrak{s}_8)^{10}$	20.947125472611013
$(10,5)$	5	$(\beta_{10,5})^2$	$(\mathfrak{s}_{10})^4$	9.249753365091010
$(11,1)$	1	$(\beta_{11,1})^{11}$	$(\mathfrak{s}_2)^{22}$	19.390218914429944
$(11,2)$	1	$(\beta_{11,2})^{11}$	$(\mathfrak{s}_4)^{22}$	31.759980453933828
$(11,3)$	1	$(\beta_{11,3})^{11}$	$(\mathfrak{s}_6)^{22}$	40.005822103105473
$(11,4)$	1	$(\beta_{11,4})^{11}$	$(\mathfrak{s}_8)^{22}$	46.083676039744226
$(11,5)$	1	$(\beta_{11,5})^{11}$	$(\mathfrak{s}_{10})^{22}$	50.873643508000555

$h_{n,p}$, where

$$\rho(g_n)=\begin{pmatrix}\cos(\frac{\pi}{n}) & -\sin(\frac{\pi}{n})\\ \sin(\frac{\pi}{n}) & \cos(\frac{\pi}{n})\end{pmatrix},$$
$$\sigma(g_n)=(1,2,\dots,2n),$$
$$\tau(g_n)=\begin{pmatrix}1 & 0\\ 0 & -1\end{pmatrix}\text{ and}$$
$$\rho(h_{n,p})=1,$$
$$\sigma(h_{n,p})=(1,3,\dots,2n-1)^{-p}(2,4,\dots,2n)^p,$$
$$\tau(h_{n,p})=\begin{pmatrix}\cos(\frac{2\pi d}{n}) & -\sin(\frac{2\pi d}{n})\\ \sin(\frac{2\pi d}{n}) & \cos(\frac{2\pi d}{n})\end{pmatrix}\quad(d:=\gcd(n,p)).$$

Let us denote by $\Lambda^G_{n,p}$, the invariant set under the action of $G_{n,p}$ in Λ, i.e.,

$$\Lambda^G_{n,p} = \{\boldsymbol{x}(t) \in \Lambda \mid x_i(t) = \rho(g)x_{\sigma(g^{-1})(i)}(\tau(g^{-1})(t)) \\ (i = 1, 2, \dots, 2n,\ g \in G_{n,p},\ t \in \mathbb{R})\}.$$

We now check the properties of $\Lambda^G_{n,p}$. First, from the invariance under g_n, we have

$$g_n \cdot ((x_1, x_2, \dots, x_{2n})(t)) = (e^{\frac{\pi i}{n}}x_{2n}, e^{\frac{\pi i}{n}}x_1, \dots, e^{\frac{\pi i}{n}}x_{2n-1})(-t).$$

Here we identify $\mathbb{R}^2$ with $\mathbb{C}$. In particular, $x_1(t), x_2(-t), \dots, x_{2n-1}(t), x_{2n}(-t)$ form a regular $2n$-gon, and n bodies with odd indices and n bodies with even indices rotate in mutually opposite directions.

Second, since

$$\rho(g_n^2) = \begin{pmatrix} \cos(\frac{2\pi}{n}) & -\sin(\frac{2\pi}{n}) \\ \sin(\frac{2\pi}{n}) & \cos(\frac{2\pi}{n}) \end{pmatrix},$$
$$\sigma(g_n^2) = (1, 3, \dots, 2n-1)(2, 4, \dots, 2n) \text{ and}$$
$$\tau(g_n^2) = 1,$$

the configuration always consists of two regular n-gons, which are formed by n bodies $x_{2i-1}(t)$'s of odd indices and n bodies $x_{2i}(t)$'s of even indices. Thus, to determine the positions of $2n$ bodies $x_1, \dots, x_{2n}$, it is sufficient to know the positions of two bodies x_1 and x_2. In fact for each $k \in \{1, \dots, n\}$ and $t \in \mathbb{R}$,

$$x_{2k-1}(t) = \omega^{(k-1)}x_1(t),\ x_{2k}(t) = \omega^{(k-1)}x_2(t),$$

where $\omega = e^{2\pi i/n}$. This enables us to use the shape sphere (introduced in Section 2.2) which represents configurations of $2n$ bodies in the periodic solutions.

Lastly, the invariance under $h_{n,p}$ tells us that

$$h_{n,p} \cdot ((x_1, x_2, \dots, x_{2n})(t)) = (x_{\sigma(h^{-1}_{n,p})(1)}, x_{\sigma(h^{-1}_{n,p})(2)}, \dots, x_{\sigma(h^{-1}_{n,p})(2n)})(t - \tfrac{dT}{n}),$$

and hence

$$x_i\left(t + \tfrac{dT}{n}\right) = x_{\sigma(h^{-1}_{n,p})(i)}(t)\ \ (i = 1, 2, \dots, 2n),$$

where

$$\sigma(h^{-1}_{n,p}) = (1, 3, \dots, 2n-1)^p(2, 4, \dots, 2n)^{-p} \in \mathfrak{S}_{2n}. \tag{2.1}$$

This implies that $\boldsymbol{x}_{n,p}(t)$ consists of $2d$ closed curves and $\frac{n}{d}$ bodies chase one another along each closed curve. See Figure 1.

2.2. **The shape sphere.** We consider the group action on the circle S^1 to $\mathbb{C}^2$ by

$$z \cdot (x_1, x_2) = (zx_1, zx_2),\ z \in S^1, (x_1, x_2) \in \mathbb{C}^2.$$

Notice that (x_1, x_2) is equivalent to (y_1, y_2) if $z \cdot (x_1, x_2) = (y_1, y_2)$ for some $z \in S^1$. The quotient space $(\mathbb{C}^2 - \{0\})/S^1$ under the above action is realized by the following projection:

$$\begin{aligned} \pi \colon \mathbb{C}^2 - \{0\} &\longrightarrow \mathbb{R}^3 - \{0\} \ (\cong (\mathbb{C}^2 - \{0\})/S^1) \\ (x_1, x_2) &\longmapsto \boldsymbol{u}(t) = (u_1, u_2, u_3) \end{aligned}$$

where

$$\begin{aligned} (u_1, u_2, u_3) &= (|x_1|^2 - |x_2|^2, 2\mathrm{Re}(x_1\bar{x_2}), 2\mathrm{Im}(x_1\bar{x_2})) \\ &= (r_1^2 - r_2^2, 2r_1r_2\cos(\theta_1 - \theta_2), 2r_1r_2\sin(\theta_1 - \theta_2)). \end{aligned}$$

Here $x_1 = r_1e^{i\theta_1}$ and $x_2 = r_2e^{i\theta_2}$. Since $x_1(t)$, $x_2(t)$ determine the solution curve, the curve $\boldsymbol{u}(t) = \pi(x_1(t), x_2(t)) \in \mathbb{R}^3$ determines this solution curve *modulo rotation*. Set the rays

$$\begin{aligned} \mathrm{A}_\pm &= \{(\pm s, 0, 0) \mid s \in \mathbb{R}_{>0}\}, \\ \mathrm{B}_{2k} &= \left\{ \left(0, s\cos(\frac{2\pi k}{n}), s\sin(\frac{2\pi k}{n}) \mid s \in \mathbb{R}_{>0} \right) \right\} \ (k \in \mathbb{Z}) \text{ and} \\ \mathrm{B}_{2k-1} &= \left\{ \left(0, s\cos(\frac{(2k-1)\pi}{n}), s\sin(\frac{(2k-1)\pi}{n}) \mid s \in \mathbb{R}_{>0} \right) \right\} \ (k \in \mathbb{Z}). \end{aligned}$$

In the quotient space $(\mathbb{C}^2 - \{0\})/S^1$, the sets $\mathrm{A}_\pm$ and B_{2k} correspond to collisions of the original $2n$ bodies. If $\boldsymbol{u}(t) \in \mathrm{A}_+$ (resp. A_-), then all bodies with odd (resp. even) indices collide at $t \in \mathbb{R}$ and if $\boldsymbol{u}(t) \in \mathrm{B}_{2k}$, then two regular n-gons fit. See Figure 4 for the configurations of 8 bodies corresponding to B_0, B_2, B_4 and B_6.

Let $\boldsymbol{u}(t)(= \boldsymbol{u}_{n,p}(t))$ be a curve corresponding to the solution $\boldsymbol{x}_{n,p}(t)$. As a result, $\boldsymbol{u}(t)$ passes through neither $\mathrm{A}_\pm$ nor B_{2k}, because $\boldsymbol{x}_{n,p}(t)$ has no collision ([Shi06, Proposition 3]). On the other hand, each B_{2k-1} represents a configuration where $2n$ bodies form a regular $2n$-gon. See Figure 4 for the configurations of 8 bodies corresponding to B_{-1}, B_1, B_3 and B_5.

Set

$$M(k) = \begin{pmatrix} -1 & 0 & 0 \\ 0 & \cos(\frac{2\pi k}{n}) & \sin(\frac{2\pi k}{n}) \\ 0 & \sin(\frac{2\pi k}{n}) & -\cos(\frac{2\pi k}{n}) \end{pmatrix}.$$

It is easy to see that $M(k)$ is an orthogonal matrix with eigenvalues $\lambda = 1, -1$. The eigenvector for $\lambda = 1$ is B_k, and hence $M(k)$ represents π-rotation with respect to B_k. The invariance under g_n is associated with

$$\begin{pmatrix} u_1(-t) \\ u_2(-t) \\ u_3(-t) \end{pmatrix} = M(-1) \begin{pmatrix} u_1(t) \\ u_2(t) \\ u_3(t) \end{pmatrix}$$

and it implies that $\boldsymbol{u}(t)$ and $\boldsymbol{u}(-t)$ are symmetric with respect to B_{-1}. In other words, rotating this curve π with respect to B_{-1}, $\boldsymbol{u}(t)$ coincides with

$\boldsymbol{u}(-t)$. In particular $\boldsymbol{u}(0) \in \mathrm{B}_{-1}$. Similarly, the invariance under $h_{n,p}$ is associated with

$$\begin{pmatrix} u_1(t+2\bar{T}) \\ u_2(t+2\bar{T}) \\ u_3(t+2\bar{T}) \end{pmatrix} = \begin{pmatrix} 1 & 0 & 0 \\ 0 & \cos(\frac{4\pi p}{n}) & -\sin(\frac{4\pi p}{n}) \\ 0 & \sin(\frac{4\pi p}{n}) & \cos(\frac{4\pi p}{n}) \end{pmatrix} \begin{pmatrix} u_1(t) \\ u_2(t) \\ u_3(t) \end{pmatrix},$$

where $\bar{T} = \frac{dT}{2n}$. Substituting $-(t+\bar{T})$ into t and applying the invariance under g_n, we obtain

$$\begin{pmatrix} u_1(-t+\bar{T}) \\ u_2(-t+\bar{T}) \\ u_3(-t+\bar{T}) \end{pmatrix} = M(2p-1) \begin{pmatrix} u_1(t+\bar{T}) \\ u_2(t+\bar{T}) \\ u_3(t+\bar{T}) \end{pmatrix}.$$

Taking $t = 0$ gives

$$\begin{pmatrix} u_1(\bar{T}) \\ u_2(\bar{T}) \\ u_3(\bar{T}) \end{pmatrix} = M(2p-1) \begin{pmatrix} u_1(\bar{T}) \\ u_2(\bar{T}) \\ u_3(\bar{T}) \end{pmatrix},$$

and hence $\boldsymbol{u}(t+\bar{T})$ and $\boldsymbol{u}(-t+\bar{T})$ are symmetric with respect to B_{2p-1} and $\boldsymbol{u}(\bar{T}) \in \mathrm{B}_{2p-1}$. It means that the original configuration of $2n$ bodies forms a regular $2n$-gon again at $t = \bar{T}$. Other symmetries with respect to B_{2jp-1} for $j = 2, 3, \ldots$ can be seen in the same manner.

Remark 2.1. *It is proved in* [Shi06, Proposition 5] *that* $\boldsymbol{u}(t) \notin \mathrm{B}_{2k-1}$ *for all* $t \in (0, \bar{T})$ *and* $k \in \mathbb{Z}$ *. It implies that* $\boldsymbol{x}_{n,p}(t)$ *and* $\boldsymbol{x}_{n,p'}(t)$ *are distinct smooth solutions for* $p \neq p'$ *in the sense that* $\boldsymbol{u}(\bar{T})$ *belongs to* B_{2p-1}*, that is in the sense that the configuration of the first regular* $2n$*-gon lives in the distinct* B_{2p-1} *for each* p*.*

Consider the projection from $\mathbb{R}^3 - \{0\}$ to the 2-sphere $\mathbb{S}^2$. The projective space is called the *shape sphere*. The image of $\boldsymbol{u}(t) \in \mathbb{R}^3 - \{0\}$ under the projection is also denoted by the same notation $\boldsymbol{u}(t)$, and we call a family $\{\boldsymbol{u}(t)\}_t$ (on the shape sphere) the *shape curve*. Determining the shape curve $\boldsymbol{u}(t)$ for $t \in (0, \bar{T})$, we obtain the shape curve $\boldsymbol{u}(t)$ for all $t \in \mathbb{R}$ from the above symmetries. For example, we show the shape curves $\boldsymbol{u}(t)$ for $t \in \mathbb{R}$ when $(n, p) = (3, 1)$ and $(n, p) = (4, 2)$ in Figure 2. Each point B_i in Figure 2 indicates the projection of the ray B_i onto the shape sphere. The solid arrows (resp. the dotted arrows) illustrate the shape curve $\boldsymbol{u}(t)$ in the front side on the shape sphere, i.e., $u_1(t)(= |x_1(t)|^2 - |x_2(t)|^2) > 0$, (resp. the back side, i.e., $u_1(t) < 0$). The dotted arrow of label 2 follows from the symmetry of the solid arrow of label 1 with respect to B_1. The remaining cases are treated in the same fashion.

Remark 2.2. *Though the set* $\Lambda^G_{n,p}$ *does not determine how the shape curve* $\boldsymbol{u}(t)$ *moves on the shape sphere for* $t \in (0, \bar{T})$*, we can prove through variational arguments that it does not happen like Figure 3(1) or (2). See* [Shi06, Propositions 5 and 6] *for the proof.*

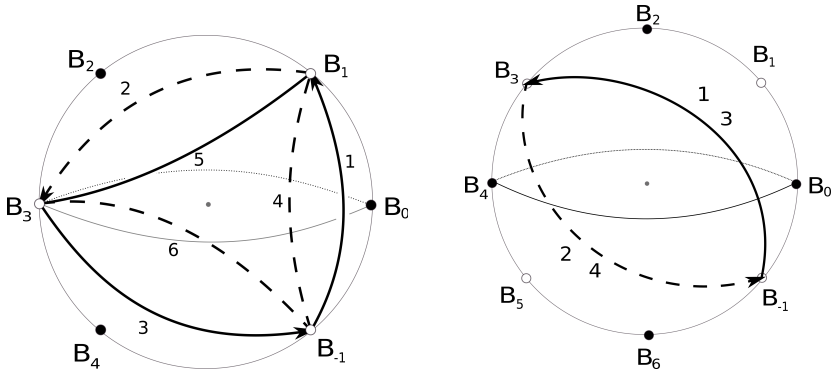

(1) $(n,p)=(3,1)$ **(2)** $(n,p)=(4,2)$

Figure 2. The shape curve $\boldsymbol{u}(t)$ for $t\in\mathbb{R}$ when (1) $(n,p)=(3,1)$ and (2) $(n,p)=(4,2)$.

The point B_i in the figure is the projection of the ray B_i onto the shape sphere.

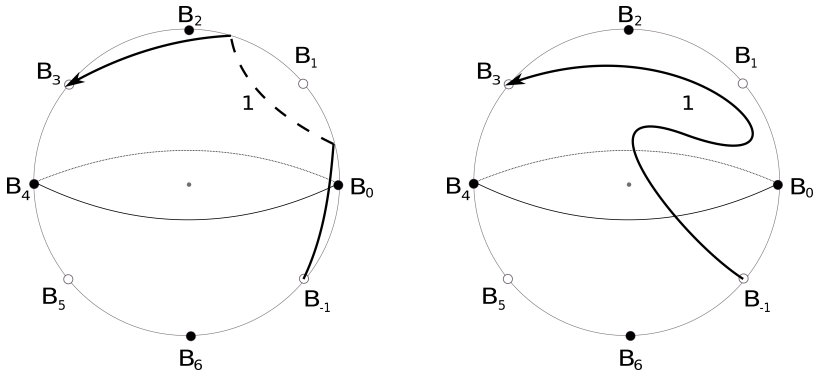

(1) Error type 1: Across the u_2u_3-plane **(2)** Error type 2: Non-monotonicity

Figure 3. Error types of the shape curve $\boldsymbol{u}(t)$ $(0\le t\le \bar{T})$ when $(n,p)=(4,2)$. (1) Error type 1: $\boldsymbol{u}(t)$ $(0\le t\le \bar{T})$ is across the u_2u_3-plane. (2) Error type 2: $\boldsymbol{u}(t)$ is not monotone. For the shape curve $\boldsymbol{u}(t)$ $(0\le t\le \bar{T})$, see the solid arrow with label 1 in Figure 2(2).

Figure 4 illustrates the projection of the shape curve $\boldsymbol{u}(t)$ onto the u_2u_3-plane together with the configuration of 8 bodies corresponding to each B_i when $(n,p)=(4,1)$ and $(4,2)$.

3. Braid groups and mapping class groups

3.1. **Geometric braids.**

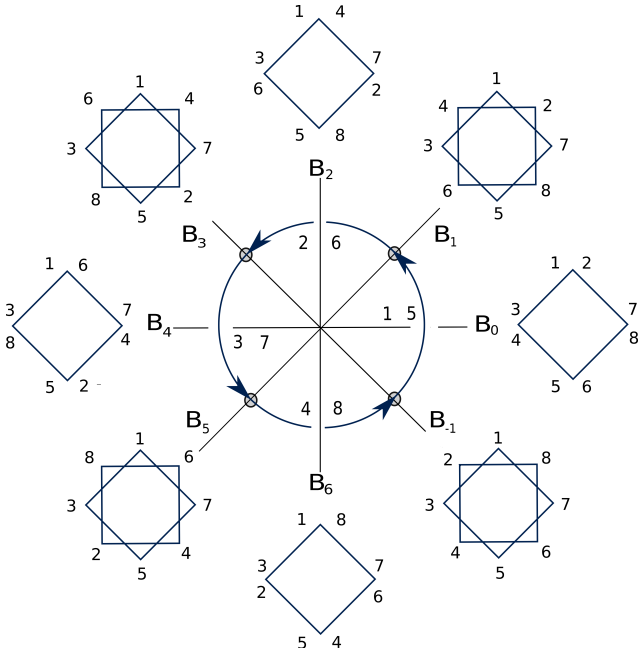

(1) $(n, p) = (4, 1)$

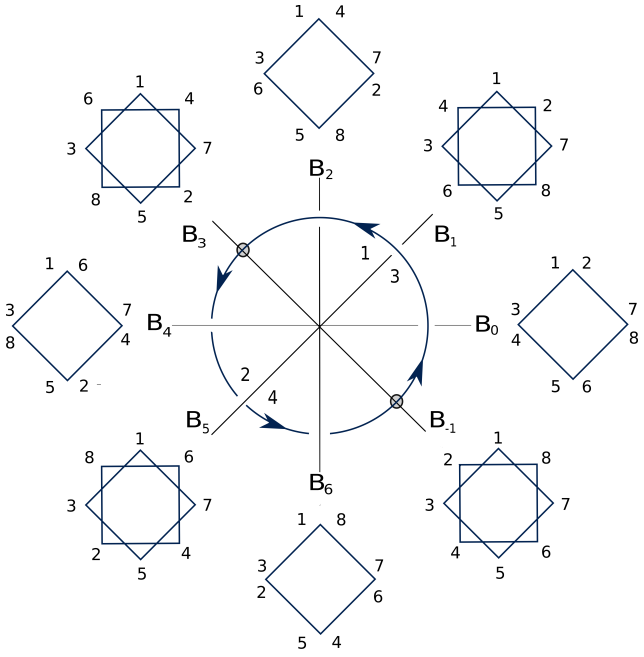

(2) $(n, p) = (4, 2)$

Figure 4. The projection of the shape curve $\boldsymbol{u}(t)$ for $t \in \mathbb{R}$ onto the u_2u_3-plane when (1) $(n, p) = (4, 1)$ and (2) $(n, p) = (4, 2)$. The configuration of 8 bodies corresponding to B_i is illustrated.

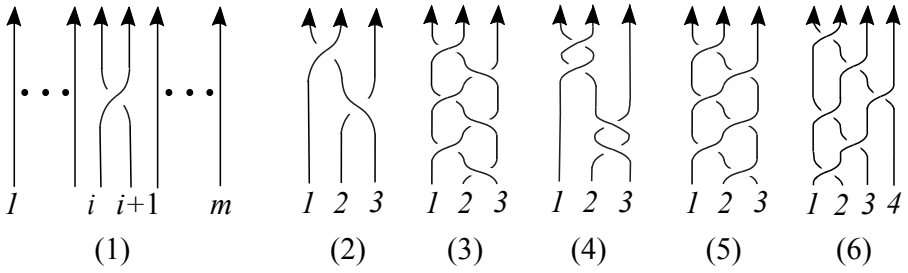

Figure 5. (1) $\sigma_i \in B_m$. (2) $\sigma_1\sigma_2^{-1} \in B_3$. (3) $(\sigma_1\sigma_2^{-1})^3 \in P_3 < B_3$. (4) $\sigma_1^2\sigma_2^{-2} \in P_3 < B_3$. (5) A full twist $\Delta^2 \in P_3 < B_3$. (6) A half twist $\Delta \in B_4$.

In this section, we recall definitions of (geometric) braids and the braid types. For the basics on braid groups, see Birman [Bir74]. Let D be a closed disk in the plane $\mathbb{R}^2$ and $Q_m = \{q_1, \dots, q_m\}$ be a set of m points in the interior of D. Let $\gamma_1, \dots, \gamma_m$ be mutually disjoint m arcs in $D \times [0,1]$ with the following properties.

- $\partial\gamma_1 \cup \cdots \cup \partial\gamma_m = \{(q_1, t), \dots, (q_m, t) \mid t \in \{0,1\}\} \subset D \times \{0,1\}$,
- γ_i $(i = 1, \dots, m)$ starts at $(q_i, 0) = \gamma_i \cap (D \times \{0\})$ and it goes up monotonically with respect to the $[0,1]$-factor. In particular $\gamma_i \cap (D \times \{t\})$ consists of a single point for $0 \le t \le 1$.

We call $b = \gamma_1 \cup \cdots \cup \gamma_m \subset D \times [0,1]$ a *(geometric) braid with base points* Q_m and call each γ_i a *strand* of the braid b. We say that braids b and b' with base points Q_m are *equivalent* if there is a 1-parameter family of braids with base points Q_m deforming b to b'. By abuse of notations, the equivalence class $[b]$ is also denoted by b.

For braids b and b' with base points Q_m, the product bb' is defined as follows. We first stuck b on b' and concatenate them to get disjoint arcs properly embedded in $D \times [0,2]$. By normalizing its height, we obtain a braid (in $D \times [0,1]$) with the same base points Q_m and this is the braid bb'. The set of all braids with base points Q_m with this product gives a group structure. The group is called the *(geometric) braid group with base points* Q_m and it is denoted by $B(Q_m)$. Note that the identity element $1_{Q_m} \in B(Q_m)$ is given by a braid consisting of straight arcs.

Let $A_m = \{a_1, \dots, a_m\}$ be a set of m points in the interior of D such that $a_1, \dots, a_m$ lie on a segment in this order. We write $B_m = B(A_m)$ and call B_m the *m-braid group*. The isomorphism class of the above braid group $B(Q_m)$ with base points Q_m does not depend on the location of base points, and $B(Q_m)$ is isomorphic to B_m. To define braid types of geometric braids with arbitrary base points Q_m, we now take an isomorphism between $B(Q_m)$ and B_m. We first choose an orientation preserving homeomorphism $f : D \to D$ such that $f(A_m) = Q_m$. Then take an isotopy $\{f_t\}_{0 \le t \le 1}$ on D between the identity map id_D and f, i.e., $f_0 = \mathrm{id}_D$ and $f_1 = f$. We consider two kinds of mutually disjoint m arcs γ^+ and γ^- properly embedded in $D \times [0,1]$ as

follows.

$$\begin{aligned}\gamma^+ &= \bigcup_{t\in[0,1]} \big\{(f_t(a_1),t),\dots,(f_t(a_m),t)\big\},\\ \gamma^- &= \bigcup_{t\in[0,1]} \big\{(f_{1-t}(a_1),t),\dots,(f_{1-t}(a_m),t)\big\}.\end{aligned}$$

Note that

$$\begin{aligned}Q_m = f_1(A_m) &= \{f(a_1),\dots,f(a_m)\} \text{ and}\\ A_m = f_0(A_m) &= \{a_1,\dots,a_m\}.\end{aligned}$$

Because of this, it makes sense to stack a braid $b \in B(Q_m)$ on γ^+, and we obtain the resulting disjoint m arcs $b\cdot\gamma^+ \subset D\times[0,2]$. Then we stack γ^- on $b\cdot\gamma^+$. As a result we have disjoint m arcs

$$\gamma^-\cdot b\cdot\gamma^+ \subset D\times[0,3].$$

By normalizing the height of the arcs, we obtain a braid (in $D\times[0,1]$) with base points A_m, and we still denote it by the same notation $\gamma^-\cdot b\cdot\gamma^+$. In particular if $b = 1_{Q_m} \in B(Q_m)$, then $\gamma^- 1_{Q_m}\gamma^+ = 1_{A_m} \in B_m$. The correspondence $b \mapsto \gamma^-\cdot b\cdot\gamma^+$ gives us an isomorphism between $B(Q_m)$ and B_m.

For an element $b \in B_m$, we put indices $1,\dots,m$ at the bottoms of strands so that the index i indicates $(a_i,0) \in D\times\{0\}$. Let σ_i be an element of B_m as in Figure 5(1). The braid group B_m is generated by $\sigma_1,\sigma_2,\dots,\sigma_{m-1}$, and it has the following braid relations.

(B1) $\sigma_i\sigma_j = \sigma_j\sigma_i$ $(|i-j|\geq 2)$.

(B2) $\sigma_i\sigma_{i+1}\sigma_i = \sigma_{i+1}\sigma_i\sigma_{i+1}$ $(1\leq i\leq m-2)$.

See Figure 5(2)–(6) for some braids. There is a surjective homomorphism

$$\hat{\sigma} : B_m \to \mathfrak{S}_m$$

from B_m to the symmetry group $\mathfrak{S}_m$ of m elements sending each σ_j to the transposition $(j,j+1)$.

Definition 3.1. *The kernel of $\hat{\sigma}$ is called the pure braid group (or colored braid group) $P_m < B_m$. An element of P_m is called a pure braid. See Figure 5(3)(4)(5) for some pure braids.*

Let $Z(B_m)$ be the center of B_m which is an infinite cyclic group generated by a *full twist* Δ^2, where a *half twist* $\Delta = \Delta_m \in B_m$ is given by

$$\Delta_m = (\sigma_1\sigma_2\dots\sigma_{m-1})(\sigma_1\sigma_2\dots\sigma_{m-2})\dots(\sigma_1\sigma_2)\sigma_1.$$

See Figure 5(6) for a half twist $\Delta \in B_4$. We note that the full twist $\Delta^2 \in B_m$ is obtained by rotating the set of m points A_m one full revolution.

We now define braid types for elements of the braid groups. Braid types were introduced originally by Boyland [Boy94, Section 9.2] as an algebraic specification of periodic orbits for surface automorphisms. See also [dCH02, Section 2.1] for a review of the study on braid types.

Definition 3.2. *For any braid $b \in B_m$ (with base points A_m), consider the projection $\overline{b}$ in the projective braid group $\mathcal{B}_m = B_m/Z(B_m)$*

$$\begin{array}{rcl} B_m & \to & \mathcal{B}_m \\ b & \mapsto & \overline{b}. \end{array}$$

The braid type $\langle b \rangle$ of b is a conjugacy class of $\overline{b}$ in the projective braid group $\mathcal{B}_m$.

In the case of the braid group $B(Q_m)$ with base points Q_m, the *braid type* $\langle b \rangle$ of $b \in B(Q_m)$ is defined by the braid type $\left\langle \gamma^- \cdot b \cdot \gamma^+ \right\rangle$ of the braid $\gamma^- \cdot b \cdot \gamma^+ \in B_m$ (with base points A_m), where γ^+ and γ^- are arcs as above. The braid type $\langle b \rangle$ is well-defined, i.e., it does not depend on the above orientation preserving homeomorphism $f : D \to D$ and the isotopy $\{f_t\}_{0 \le t \le 1}$.

Example 3.3.

(1) *For the 3-braid $\sigma_1 \sigma_2^{-1}$, it follows that*

$$\hat{\sigma}(\sigma_1 \sigma_2^{-1}) = \hat{\sigma}(\sigma_1)\hat{\sigma}(\sigma_2^{-1}) = (12)(23) = (123) \in \mathfrak{S}_3,$$

see Figure 5(2). Hence $\hat{\sigma}((\sigma_1 \sigma_2^{-1})^3) = 1 \in \mathfrak{S}_3$ which means that $(\sigma_1 \sigma_2^{-1})^3 \in P_3$.

(2) *For the 3-braid $\sigma_1^2 \sigma_2^{-2}$, it follows that*

$$\hat{\sigma}(\sigma_1^2 \sigma_2^{-2}) = \hat{\sigma}(\sigma_1^2)\hat{\sigma}(\sigma_2^{-2}) = 1 \cdot 1 = 1 \in \mathfrak{S}_3,$$

see Figure 5(4). Hence $\sigma_1^2 \sigma_2^{-2} \in P_3$.

Example 3.4. *For Euler's periodic solution of the planar 3-body problem, three bodies are collinear at every instant. A full twist $\Delta^2 = (\sigma_1 \sigma_2 \sigma_1)^2 = (\sigma_1 \sigma_2)^3 \in B_3$ (Figure 5(5)) represents the braid type of the solution. Since $Z(B_3)$ is generated by Δ^2, the braid type of Euler's periodic solution is trivial in $\mathcal{B}_3 = B_3/Z(B_3)$. Similarly, it is the trivial braid type for Lagrange's periodic solution of the planar 3-body problem, since the triangle formed by the three bodies is equilateral for all time and the 3-braid obtained by rotating a triangle one full revolution is a full twist.*

3.2. **Mapping class groups.** Let $X_1, \ldots, X_n$ be possibly empty subspaces of an orientable manifold M. For instance M is a connected orientable surface $\Sigma_{g,m}$ of genus $g \ge 0$ with m punctures (possibly $m = 0$) and X_i $(i = 1, \ldots, n)$ is a finite set in $\Sigma_{g,m}$. Let $\mathrm{Homeo}_+(M, X_1, \ldots, X_n)$ be the group of orientation-preserving self-homeomorphisms of M that map X_i onto X_i for each $i = 1, \ldots, n$. We do not require that homeomorphisms fix the boundary ∂M pointwise. The mapping class group $\mathrm{MCG}(M, X_1, \ldots, X_n)$ is defined by

$$\mathrm{MCG}(M, X_1, \ldots, X_n) = \pi_0(\mathrm{Homeo}_+(M, X_1, \ldots, X_n)),$$

that is the group of isotopy classes of elements of $\mathrm{Homeo}_+(M, X_1, \ldots, X_n)$. When X is an empty subspace of M, then we write $\mathrm{MCG}(M) = \mathrm{MCG}(M, X)$.

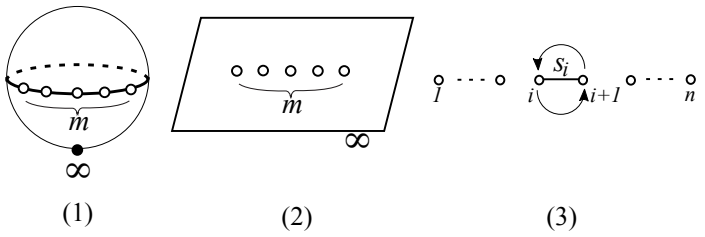

Figure 6. (1) A pair $(\Sigma_{0,m}, \{\infty\})$. (2) An m-punctured plane. (3) A half twist h_i.

We apply elements of mapping class groups from right to left, i.e., we apply g first for the product fg.

Let $D_m = D \setminus A_m$ be an m-punctured disk, where $A_m = \{a_1, \ldots, a_m\}$ is the set of m points in the interior of D as in Section 3.1. By definition, $\mathrm{MCG}(D_m)$ is the group of isotopy classes of elements of $\mathrm{Homeo}_+(D_m)$ which fix ∂D setwise. In this paper, we mainly consider an m-punctured disk D_m or an m-punctured sphere $\Sigma_{0,m}$ as an orientable manifold M for the mapping class groups. We take a point in $\Sigma_{0,m}$ and call it ∞. An element $f \in \mathrm{Homeo}_+(\Sigma_{0,m}, \{\infty\})$ means that f fixes the point ∞. Puncturing the point ∞, we think of $\mathrm{MCG}(\Sigma_{0,m}, \{\infty\})$ as a subgroup of $\mathrm{MCG}(\Sigma_{0,m+1})$. Also we may regard $\mathrm{MCG}(\Sigma_{0,m}, \{\infty\})$ as the mapping class group of an m-punctured plane. See Figure 6(1)(2).

The mapping class group $\mathrm{MCG}(D_m)$ is generated by $h_1, \ldots, h_{m-1}$, where h_i is the right-handed *half twist* about a segment s_i connecting the ith and $(i+1)$th punctures, see Figure 6(3). More precisely, let $\mathbb{D}_i \subset \mathrm{int}(D)$ be a closed disk such that $\mathbb{D}_i$ contains the two points a_i and a_{i+1} together with a segment s_i between the punctures a_i and a_{i+1}. Moreover $\mathbb{D}_i$ contains no other points of A_m. Then the right-handed half-twist $h_i \in \mathrm{MCG}(D_m)$ is a mapping class that fixes the exterior of $\mathbb{D}_i$ and rotates s_i in $\mathbb{D}_i$ by π in the counter-clockwise direction. Hence h_i interchanges the ith puncture with the $(i+1)$th puncture.

We now recall a relation between B_m and $\mathrm{MCG}(D_m)$. There is a surjective homomorphism

$$\Gamma : B_m \to \mathrm{MCG}(D_m)$$

which sends σ_i to h_i for $i = 1, \ldots, m-1$. The kernel of Γ is the center $Z(B_m)$, and hence $\mathcal{B}_m = B_m/Z(B_m)$ is isomorphic to $\mathrm{MCG}(D_m)$. Collapsing ∂D to the point ∞ in the sphere, we have a homomorphism

$$\mathfrak{c} : \mathrm{MCG}(D_m) \to \mathrm{MCG}(\Sigma_{0,m}, \{\infty\}).$$

By abuse of notations, we simply denote by b, the mapping class $\mathfrak{c}(\Gamma(b)) \in \mathrm{MCG}(\Sigma_{0,m}, \{\infty\})$. Also we denote by $\langle b \rangle$, the conjugacy class $\langle \mathfrak{c}(\Gamma(b)) \rangle$ of $\mathfrak{c}(\Gamma(b)) \in \mathrm{MCG}(\Sigma_{0,m}, \{\infty\})$. Note that this notation $\langle b \rangle$ is the same as the braid type of $b \in B_m$.

3.3. **Nielsen-Thurston classification.** According to the Nielsen-Thurston classification [Thu88], mapping classes fall into three types: periodic, reducible and pseudo-Anosov. Assume that $3g-3+m \geq 1$. A mapping class $\phi \in \mathrm{MCG}(\Sigma_{g,m})$ is *periodic* if ϕ is of finite order. A mapping class $\phi \in \mathrm{MCG}(\Sigma_{g,m})$ is *reducible* if there is a collection of mutually disjoint and non-homotopic essential simple closed curves $C_1, \ldots, C_j$ in $\Sigma_{g,m}$ for $j \geq 1$ such that $C_1 \cup \cdots \cup C_j$ is preserved by ϕ. Here a simple closed curve C in $\Sigma_{g,m}$ is *essential* if it is not homotopic to a point. (There is a mapping class that is periodic and reducible.) A mapping class $\phi \in \mathrm{MCG}(\Sigma_{g,m})$ is *pseudo-Anosov* if ϕ is neither periodic nor reducible. Note that the Nielsen-Thurston type is a conjugacy invariant, i.e., two mapping classes are conjugate to each other in $\mathrm{MCG}(\Sigma_{g,m})$, then their Nielsen-Thurston types are the same.

Pseudo-Anosov mapping classes have many important properties for the study of dynamical systems. For more details which we describe below, see [FLP79, FM12]. A homeomorphism $\Phi : \Sigma_{g,m} \to \Sigma_{g,m}$ is *pseudo-Anosov* if there exist a constant $\lambda = \lambda(\Phi) > 1$ and a pair of transverse measured foliations $(\mathcal{F}^+, \mu^+)$ and $(\mathcal{F}^-, \mu^-)$ such that

$$\Phi((\mathcal{F}^+, \mu^+)) = (\mathcal{F}^+, \lambda\mu^+) \quad \textit{and} \quad \Phi((\mathcal{F}^-, \mu^-)) = (\mathcal{F}^-, \tfrac{1}{\lambda}\mu^-).$$

This means that Φ preserves both foliations $\mathcal{F}^+$ and $\mathcal{F}^-$, and it contracts the leaves of $\mathcal{F}^-$ by $\frac{1}{\lambda}$ and it expands the leaves of $\mathcal{F}^+$ by λ. The invariant foliations $\mathcal{F}^+$ and $\mathcal{F}^-$ are called the *unstable and stable foliations* for Φ, and $\lambda > 1$ is called the *stretch factor* for Φ.

Remark 3.5. *The invariant foliations $\mathcal{F}^+$ and $\mathcal{F}^-$ for the pseudo-Anosov homeomorphism Φ are singular foliations which mean that they have common singularities in the interior of $\Sigma_{g,m}$ or at punctures of $\Sigma_{g,m}$. The number of singularities is finite. A 1-pronged singularity may occur at a puncture of $\Sigma_{g,m}$, yet there are no 1-pronged singularities in the interior of $\Sigma_{g,m}$.*

Each pseudo-Anosov mapping class $\phi \in \mathrm{MCG}(\Sigma_{g,m})$ contains a pseudo-Anosov homeomorphism Φ as a representative of ϕ. We set $\lambda(\phi) = \lambda(\Phi)$ and call it the *stretch factor* of the mapping class $\phi = [\Phi]$. The stretch factor $\lambda(\phi)$ is a conjugacy invariant of pseudo-Anosov mapping classes. Moreover $\lambda(\phi)$ is the largest eigenvalue of a Perron-Frobenius integral matrix. Thus $\lambda(\phi)$ is an algebraic integer which is a real number greater than 1 and $|\lambda'| < \lambda(\phi)$ holds for each conjugate element $\lambda' \neq \lambda(\phi)$. The logarithm $\log(\lambda(\phi))$ of the stretch factor $\lambda(\phi)$ is called the *entropy* of ϕ.

Remark 3.6. *If $\phi \in \mathrm{MCG}(\Sigma_{g,m})$ is pseudo-Anosov, then ϕ^k is pseudo-Anosov for all $k \geq 1$ and the equality $\lambda(\phi^k) = (\lambda(\phi))^k$ holds.*

Recall the two homomorphisms $\Gamma : B_m \to \mathrm{MCG}(D_m)$ and $\mathfrak{c} : \mathrm{MCG}(D_m) \to \mathrm{MCG}(\Sigma_{0,m}, \{\infty\}) < \mathrm{MCG}(\Sigma_{0,m+1})$. We say that a braid $b \in B_m$ is *periodic* (resp. *reducible*, *pseudo-Anosov*) if the mapping class $\mathfrak{c}(\Gamma(b))$ is of the corresponding type. When b is a pseudo-Anosov braid, the *stretch factor* $\lambda(b)$

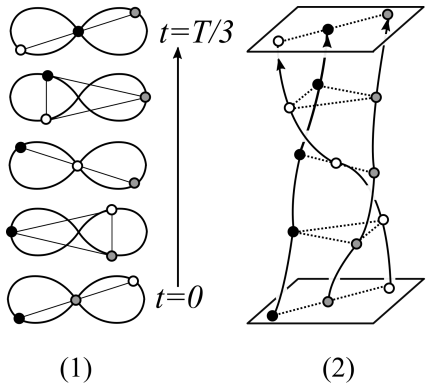

Figure 7. (1) The figure-8 solution $\boldsymbol{x}(t)$ with period T. (2) A representative braid $\sigma_1^{-1}\sigma_2 \in \langle b(\boldsymbol{x}(t), [0, \frac{T}{3}])\rangle$.

of b is defined by the stretch factor $\lambda(\mathfrak{c}(\Gamma(b)))$ of the mapping class $\mathfrak{c}(\Gamma(b))$. In this case, it makes sense to say that the braid type $\langle b\rangle$ is *pseudo-Anosov* (see Definition 3.2 for the definition of braid types), and we can define the *stretch factor* $\lambda(\langle b\rangle)$ of the braid type $\langle b\rangle$ by

$$\lambda(\langle b\rangle) = \lambda(b) = \lambda(\mathfrak{c}(\Gamma(b))), \tag{3.1}$$

since both Nielsen-Thurston type and the stretch factor are conjugacy invariants.

3.4. **Pseudo-Anosov 3-braids.** It is well-known that for positive integers k_j's, ℓ_j's, r and an integer s, the 3-braid

$$\Delta^{2s}\sigma_1^{k_1}\sigma_2^{-\ell_1}\dots\sigma_1^{k_r}\sigma_2^{-\ell_r}$$

is pseudo-Anosov. Moreover any pseudo-Anosov 3-braid α is conjugate to a braid $\Delta^{2s}\sigma_1^{k_1}\sigma_2^{-\ell_1}\dots\sigma_1^{k_r}\sigma_2^{-\ell_r}$ in B_3 which is unique up to a cyclic permutation. See Murasugi [Mur74, Proposition 2.1], Handel [Han97, Lemma 0.1] for example. Then the stretch factor $\lambda(\alpha)$ is the eigenvalue greater than 1 of

$$M_{(k_1,\ell_1,\dots,k_r,\ell_r)} = \begin{pmatrix}1 & 1\\ 0 & 1\end{pmatrix}^{k_1}\begin{pmatrix}1 & 0\\ 1 & 1\end{pmatrix}^{\ell_1}\cdots\begin{pmatrix}1 & 1\\ 0 & 1\end{pmatrix}^{k_r}\begin{pmatrix}1 & 0\\ 1 & 1\end{pmatrix}^{\ell_r}. \tag{3.2}$$

See Handel [Han97].

Example 3.7 (Metallic 3-braids (Appendix A in [FT11]))**.** *For $p \geq 1$, the 3-braid $\sigma_1^{2p}\sigma_2^{-2p}$ is pseudo-Anosov, and the stretch factor $\lambda(\sigma_1^{2p}\sigma_2^{-2p})$ is the eigenvalue greater than 1 of $M_{(2p,2p)} = \begin{pmatrix}1+4p^2 & 2p\\ 2p & 1\end{pmatrix}$. Thus*

$$\lambda(\sigma_1^{2p}\sigma_2^{-2p}) = (p+\sqrt{p^2+1})^2 = \Big(\frac{1}{2}(2p+\sqrt{4p^2+4})\Big)^2 = (\mathfrak{s}_{2p})^2.$$

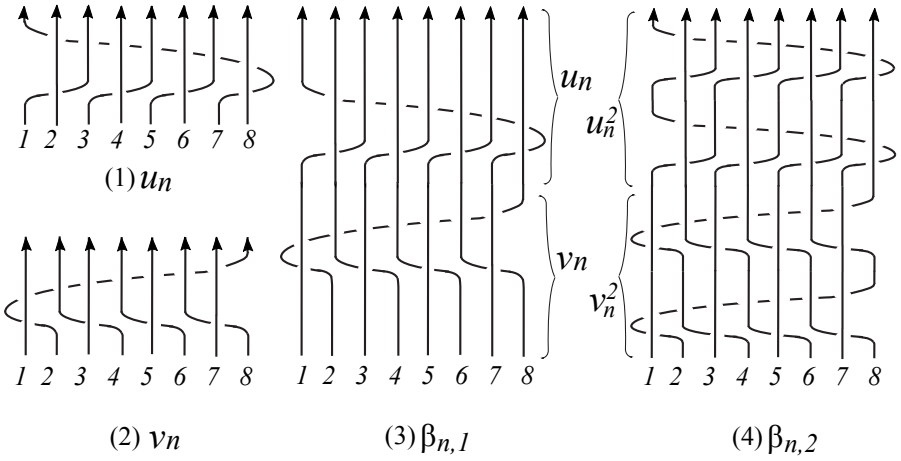

Figure 8. Case $n = 4$. (1) u_n. (2) v_n. (3) $\beta_{n,1} = u_n v_n$. (4) $\beta_{n,2} = u_n^2 v_n^2$.

Example 3.8. *Let us consider the figure-*8 *solution* $\boldsymbol{x}(t) = (x_1(t), x_2(t), x_3(t))$ *by Moore* [Moo93] *and Chenciner-Montgomery* [CM00]*, see Figure 7. The periodic solution* $\boldsymbol{x}(t)$ *has a property such that*

$$x_1(t + \tfrac{T}{3}) = x_2(t), \;\; x_2(t + \tfrac{T}{3}) = x_3(t), \;\; x_3(t + \tfrac{T}{3}) = x_1(t),$$

where $T > 0$ *is the period of* $\boldsymbol{x}(t)$*. This property tells us that* $\boldsymbol{x}(t)$ *determines a braid* $b(\boldsymbol{x}(t), [0, \frac{T}{3}])$*. One sees that* $\sigma_1^{-1}\sigma_2 \in B_3$ *is a representative of* $\langle b(\boldsymbol{x}(t), [0, \frac{T}{3}]) \rangle$ *and* $(\sigma_1^{-1}\sigma_2)^3$ *represents the braid type* $\langle b(\boldsymbol{x}(t), [0, T]) \rangle$ *of the solution* $\boldsymbol{x}(t)$*. It is easy to see that* $\sigma_1^{-1}\sigma_2$ *is conjugate with* $\sigma_1\sigma_2^{-1}$ *in* B_3*. By* (3.2)*,* $\sigma_1\sigma_2^{-1}$ *is a pseudo-Anosov braid with the stretch factor* $(\mathfrak{s}_1)^2$*. Thus the braid type of the figure-*8 *solution is pseudo-Anosov with the stretch factor* $(\mathfrak{s}_1)^6$ *(Remark 3.6), and hence it is a non-trivial braid type in contrast with the Euler's solution and Lagrange's solution (Example 3.4).*

4. Proof of Theorem 1.5

For $n \geq 2$ and $p \geq 1$, we define braids $u_n, v_n, \beta_{n,p} \in B_{2n}$ as follows.

$$\begin{aligned} u_n &= (\sigma_1\sigma_2 \dots \sigma_{2n-1})(\sigma_1\sigma_3 \dots \sigma_{2n-1})^{-1}, \\ v_n &= (\sigma_1\sigma_2 \dots \sigma_{2n-1})^{-1}(\sigma_1\sigma_3 \dots \sigma_{2n-1}) \text{ and} \\ \beta_{n,p} &= u_n^p v_n^p. \end{aligned}$$

See also Figure 8 together with the braid relation (B1) in Section 3.1. It is easy to check that $\hat{\sigma}(u_n) = (1, 3, \dots, 2n-1)$ and $\hat{\sigma}(v_n) = (2, 4, \dots, 2n)^{-1}$. Hence by (2.1), we have

$$\hat{\sigma}(\beta_{n,p}) = \hat{\sigma}(u_n^p v_n^p) = (1, 3, \dots, 2n-1)^p (2, 4, \dots, 2n)^{-p} = \sigma(h_{n,p}^{-1}). \tag{4.1}$$

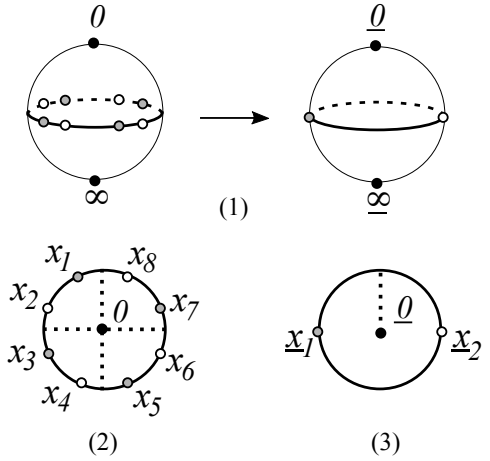

Figure 9. Case $n = 4$. (1) An n-fold branched cover $\mathfrak{p} : \Sigma_{0,2n} \to \Sigma_{0,2}$ with branched points $\underline{0}$ and $\underline{\infty}$, where punctures lie on the equators. (2) The upper hemisphere for $\Sigma_{0,2n}$. (3) The upper hemisphere for $\Sigma_{0,2}$.

Proof of Theorem 1.5. The proof consists of the following two steps. In Step 1, we prove that for $n \geq 2$ and *any* $p \geq 1$, the braid $\beta_{n,p}$ is pseudo-Anosov with $\lambda(\beta_{n,p}) = (\mathfrak{s}_{2p})^2$. (We have no restriction on p in Step 1.) In Step 2, we prove that for any $n \geq 2$ and $p \in \{1, \dots, \lfloor \frac{n}{2} \rfloor\}$, the braid types of $\beta_{n,p}$ and $y_{n,p} = b(\boldsymbol{x}_{n,p}(t), [0, \frac{d}{n}])$ are the same. In other words, $\beta_{n,p} \in \langle y_{n,p} \rangle$. Since $X_{n,p} = \langle (y_{n,p})^{\frac{n}{d}} \rangle$, it follows that $X_{n,p} = \langle (\beta_{n,p})^{\frac{n}{d}} \rangle$. Hence by Step 1 together with Remark 3.6, $X_{n,p}$ is a pseudo-Anosov braid type with the stretch factor

$$\lambda(X_{n,p}) = \lambda\big((\beta_{n,p})^{\frac{n}{d}}\big) = (\lambda(\beta_{n,p}))^{\frac{n}{d}} = (\mathfrak{s}_{2p})^{\frac{2n}{d}}.$$

Step 1. For $n \geq 2$ and $p \geq 1$, the braid $\beta_{n,p}$ is pseudo-Anosov with $\lambda(\beta_{n,p}) = (\mathfrak{s}_{2p})^2$. In particular $\lambda(\beta_{n,p}) < \lambda(\beta_{n,p'})$ if $p < p'$.

Proof of Step 1. We consider a 2-punctured sphere $\Sigma_{0,2}$ and denote the two punctures of $\Sigma_{0,2}$ by $\underline{x}_1$ and $\underline{x}_2$. We pick two points in $\Sigma_{0,2}$ and call them $\underline{0}$ (the north pole) and $\underline{\infty}$ (the south pole). Given $n \geq 2$, we take an n-fold branched cover

$$\mathfrak{p} : \Sigma_{0,2n} \to \Sigma_{0,2}$$

with branched points $\underline{0}$ and $\underline{\infty}$. (We cut a longitude of $\Sigma_{0,2}$ between $\underline{0}$ and $\underline{\infty}$, take n copies of the resulting surface, and past them to make a $2n$-punctured sphere.) We denote lifts of $\underline{0}, \underline{\infty} \in \Sigma_{0,2}$ by $0, \infty \in \Sigma_{0,2n}$ respectively. Let $x_1, x_2, \dots, x_{2n}$ be punctures of $\Sigma_{0,2n}$ such that $\mathfrak{p}$ sends x_{2k} (resp. x_{2k-1}) to

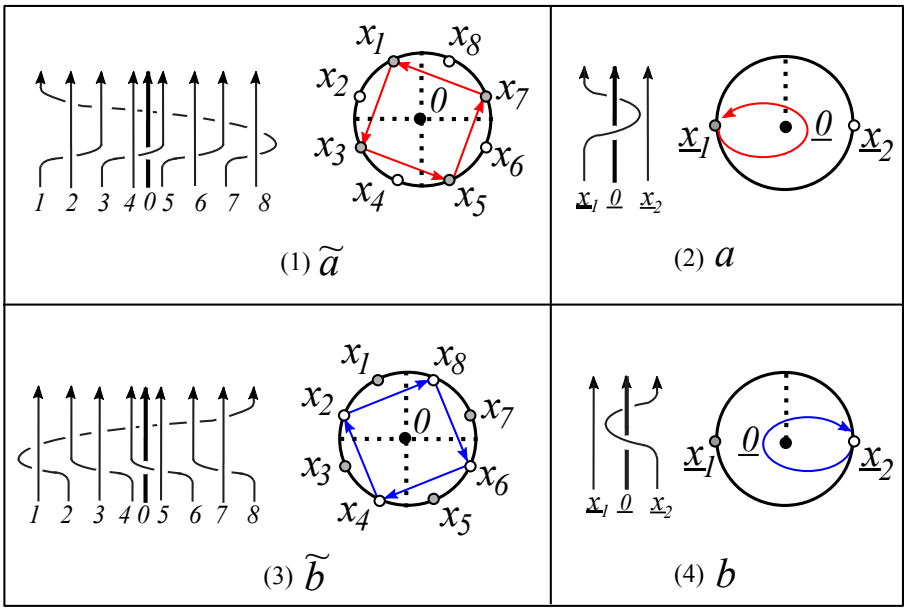

Figure 10. Case $n = 4$. (1) A lift $\widetilde{a} = \widetilde{a_n} \in \mathrm{MCG}(\Sigma_{0,2n}, \{0\}, \{\infty\})$ of (2) $a = \sigma_1^2 \in \mathrm{MCG}(\Sigma_{0,2}, \{\underline{0}\}, \{\underline{\infty}\})$. (3) A lift $\widetilde{b} = \widetilde{b_n} \in \mathrm{MCG}(\Sigma_{0,2n}, \{0\}, \{\infty\})$ of (4) $b = \sigma_2^{-2} \in \mathrm{MCG}(\Sigma_{0,2}, \{\underline{0}\}, \{\underline{\infty}\})$. For (2) and (4), a and b (as elements of B_3) have base points $\underline{x}_1$, $\underline{0}$, and $\underline{x}_2$.

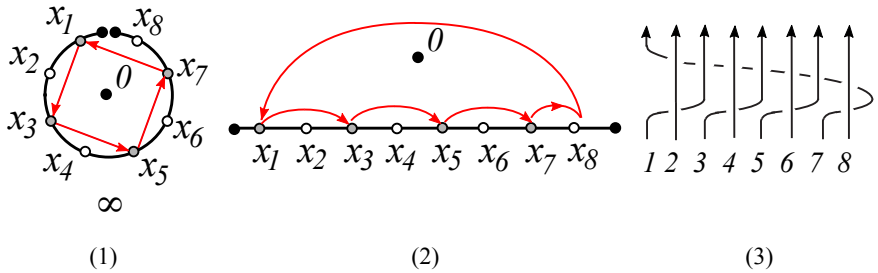

Figure 11. Case $n = 4$. (1) An arc in the equator. (2) A segment in the plane. (3) The braid u_n corresponding to $\widetilde{a}^\bullet \in \mathrm{MCG}(\Sigma_{0,2n}, \{\infty\})$. (The arc in (1) is identified with the segment in (2).) For (1) and (2), arrows indicate the image of the punctures under $\widetilde{a}$.

$\underline{x}_2$ (resp. $\underline{x}_1$). In the view from $0 \in \Sigma_{0,2n}$ in the upper hemisphere, we may assume that $x_1, \ldots, x_{2n}$ lie on the equator counterclockwise and these $2n$ punctures form the regular $2n$-gon. See Figure 9.

Let $a = \sigma_1^2$, $b = \sigma_2^{-2} \in B_3$. Since a and b are pure 3-braids, we can regard a and b as elements of $\mathrm{MCG}(\Sigma_{0,2}, \{\underline{0}\}, \{\underline{\infty}\})$, see Figure 10(2)(4). We lift a

and b to $\Sigma_{0,2n}$, and call them

$$\widetilde{a}, \widetilde{b} \in \mathrm{MCG}(\Sigma_{0,2n}, \{0\}, \{\infty\}) < \mathrm{MCG}(\Sigma_{0,2n+1}, \{\infty\}).$$

(Clearly both $\widetilde{a}$ and $\widetilde{b}$ fix the two points 0 and ∞.) We have

$$\begin{aligned} \widetilde{a}(x_{2k-1}) &= x_{2k+1} \text{ and } \widetilde{a}(x_{2k}) = x_{2k} \text{ for } k = 1, \dots, n, \\ \widetilde{b}(x_{2k-1}) &= x_{2k-1} \text{ and } \widetilde{b}(x_{2k}) = x_{2k-2} \text{ for } k = 1, \dots, n, \end{aligned}$$

where we interpret indices modulo $2n$. Notice that $\widetilde{a}$ rotates the regular n-gon $x_1 x_3 \dots x_{2n-1}$ by $\frac{\pi}{n}$ counterclockwise about the north pole 0; $\widetilde{b}$ rotates the regular n-gon $x_2 x_4 \dots x_{2n}$ by $\frac{\pi}{n}$ clockwise about the same point 0, see Figure 10(1)(3). In other words, under the action of $\widetilde{a}$, each puncture x_{2i-1} $(i = 1, \dots, 2n)$ with the odd index is passing through in front of the puncture x_{2i} with the even index from the view of the north pole $0 \in \Sigma_{0,2n}$. Similarly, under the action of $\widetilde{b}$, each puncture x_{2i} $(i = 1, \dots, 2n)$ with the even index is passing through in front of the puncture x_{2i-1} with the odd index.

Forgetting the point $0 \in \Sigma_{0,2n}$, we think of $\widetilde{a}$ and $\widetilde{b}$ as elements, say $\widetilde{a}^\bullet$ and $\widetilde{b}^\bullet$ of $\mathrm{MCG}(\Sigma_{0,2n}, \{\infty\})$ respectively. To find the planar $2n$-braids for $\widetilde{a}^\bullet$ and $\widetilde{b}^\bullet$, we cut the equator of $\Sigma_{0,2n}$ at a point between the consecutive punctures x_{2n} and x_1 (in the cyclic order) into an arc, and we regard the arc as a segment in the plane containing the punctures $x_1, \dots, x_{2n}$ in this order, see Figure 11(1)(2). Then from the actions of $\widetilde{a}^\bullet$ and $\widetilde{b}^\bullet$ on $2n$ punctures in the plane, one sees that $2n$-braids corresponding to $\widetilde{a}^\bullet$, $\widetilde{b}^\bullet$ are given by u_n, $v_n \in B_{2n}$ respectively. See Figure 11(3). (Although we do not need braid representatives corresponding to $\widetilde{a}$ and $\widetilde{b}$ in the proof of Step 1, Figure 10(1) and (3) illustrate these representatives for $\widetilde{a}$ and $\widetilde{b}$ respectively in case $n = 4$.)

We define

$$\phi_p = (\widetilde{a})^p (\widetilde{b})^p \in \mathrm{MCG}(\Sigma_{0,2n}, \{0\}, \{\infty\}) < \mathrm{MCG}(\Sigma_{0,2n+1}, \{\infty\}).$$

It follows that ϕ_p is a lift of $a^p b^p = \sigma_1^{2p} \sigma_2^{-2p} \in \mathrm{MCG}(\Sigma_{0,2}, \{\underline{0}\}, \{\underline{\infty}\})$. Recall that $a^p b^p$ is a pseudo-Anosov mapping class with the stretch factor $(\mathfrak{s}_{2p})^2$, see Example 3.7. Since ϕ_p is a lift of $a^p b^p$, ϕ_p is also pseudo-Anosov with the same stretch factor as $a^p b^p$. Hence $\lambda(\phi_p) = (\mathfrak{s}_p)^2$.

Forgetting the point $0 \in \Sigma_{0,2n}$, we obtain $\phi_p^\bullet \in \mathrm{MCG}(\Sigma_{0,2n}, \{\infty\})$ from $\phi_p = (\widetilde{a})^p (\widetilde{b})^p$. Note that $\phi_p^\bullet = (\widetilde{a}^\bullet)^p (\widetilde{b}^\bullet)^p$ is a mapping class corresponding to the braid $\beta_{n,p} = u_n^p v_n^p$.

Claim. The stable/unstable foliation $\mathcal{F}^{+/-}$ of ϕ_p is not 1-pronged at $0 \in \Sigma_{0,2n}$.

For the proof of Step 1, it is enough to prove Claim. The reason is that if $\mathcal{F}^{+/-}$ is not 1-pronged at the point $0 \in \Sigma_{0,2n}$, then the same singular foliations $\mathcal{F}^+$ and $\mathcal{F}^-$ are still invariant foliations for $\phi_p^\bullet$, see Remark 3.5.

This implies that $\phi_p^\bullet$ (and hence the braid $\beta_{n,p}$) is pseudo-Anosov with the same stretch factor $(\mathfrak{s}_p)^2$ as ϕ_p, i.e.,

$$\lambda(\beta_{n,p})\Big(=\lambda(\phi_p^\bullet)\Big)=\lambda(\phi_p)=(\mathfrak{s}_{2p})^2.$$

Proof of Claim. Let us consider the stable/unstable foliation $\underline{\mathcal{F}}^+$ and $\underline{\mathcal{F}}^-$ for the pseudo-Anosov element a^pb^p. Then $\underline{\mathcal{F}}^{+/-}$ has 1-pronged singularities at each of the two punctures of $\Sigma_{0,2}$ and at each of the two points $\underline{0}$ and $\underline{\infty}$. Let $\mathcal{F}^+$ and $\mathcal{F}^-$ denote lifts of $\underline{\mathcal{F}}^+$ and $\underline{\mathcal{F}}^-$ respectively. It follows that $\mathcal{F}^{+/-}$ is the stable/unstable foliation for ϕ_p, and $\mathcal{F}^{+/-}$ has a 1-pronged singularity at each of the $2n$ punctures and $\mathcal{F}^{+/-}$ has n-pronged singularities ($n\geq 2$) at the points 0 and ∞ in $\Sigma_{0,2n}$. In particular $\mathcal{F}^{+/-}$ is not 1-pronged at $0\in\Sigma_{0,2n}$. This completes the proof of Claim.

By Claim, we finished the proof of Step 1.

Recall that $y_{n,p}=b(\boldsymbol{x}_{n,p}(t),[0,2\bar{T}])$ and $\bar{T}=\frac{dT}{2n}$.

Step 2. $\beta_{n,p}\in\langle y_{n,p}\rangle$. In particular $(\beta_{n,p})^{\frac{n}{d}}\in X_{n,p}=\big\langle (y_{n,p})^{\frac{n}{d}}\big\rangle$.

Proof of Step 2. Let us consider the shape curve $\boldsymbol{u}(t)$ ($t\in[0,2\bar{T}]$) for the solution $\boldsymbol{x}_{n,p}(t)$. By the arguments in Section 2.2, the shape curve $\boldsymbol{u}(t)$ ($t\in[0,2\bar{T}]$) satisfies the following properties.
(s1) $\boldsymbol{u}(0)\in \mathrm{B}_{-1}$, $\boldsymbol{u}(\bar{T})\in \mathrm{B}_{2p-1}$ and $\boldsymbol{u}(2\bar{T})\in \mathrm{B}_{4p-1}$.
(s2) $u_1(t)>0$ for $0<t<\bar{T}$.
(s3) $u_1(t)<0$ for $\bar{T}<t<2\bar{T}$.
(s4) $x_i(2\bar{T})=x_{\sigma(h_{n,p}^{-1})(i)}(0)$ for $i=1,\dots,2n$.

Recall that n bodies with odd indices and n bodies with even indices rotate in mutually opposite directions. See Section 2.1. The above (s1) ($\boldsymbol{u}(0)\in \mathrm{B}_{-1}$, $\boldsymbol{u}(\bar{T})\in \mathrm{B}_{2p-1}$) and (s2) tell us that each of bodies $x_{2i}(t)$'s ($i=1,\dots,n$) with even indices is passing through in front of bodies with odd indices (in the time interval $(0,\bar{T})$) from the view of the origin $0\in\mathbb{R}^2$. Similarly (s1) ($\boldsymbol{u}(\bar{T})\in \mathrm{B}_{2p-1}$, $\boldsymbol{u}(2\bar{T})\in \mathrm{B}_{4p-1}$) and (s3) imply that each of bodies $x_{2i-1}(t)$'s ($i=1,\dots,n$) with odd indices is passing through in front of the bodies with even indices (in the time interval $(\bar{T},2\bar{T})$). These properties connect up $(\widetilde{b})^p\in \mathrm{MCG}(\Sigma_{0,2n},\{0\},\{\infty\})$ with $\boldsymbol{u}(t)$ for $t\in[0,\bar{T}]$ (resp. $(\widetilde{a})^p\in \mathrm{MCG}(\Sigma_{0,2n},\{0\},\{\infty\})$ with $\boldsymbol{u}(t)$ for $t\in[\bar{T},2\bar{T}]$), see Figure 10(3)(4). Recall that the permutation $\hat{\sigma}(\beta_{n,p})$ of the braid $\beta_{n,p}=u_n^pv_n^p$ coincides with $\sigma(h_{n,p}^{-1})$, see (4.1). Putting these properties together with (s4), we conclude that the $2n$-braid $u_n^pv_n^p(=\beta_{n,p})$ is a representative of the braid type $\langle y_{n,p}\rangle$ of $y_{n,p}=b(\boldsymbol{x}_{n,p}(t),[0,2\bar{T}])$. This completes the proof of Step 2.

By Steps 1 and 2, we have finished the proof of Theorem 1.5. □

We end this section with an example.

Example 4.1. *Corollary 1.6 and Table 1 may suggest that $\lambda(X_{n,p})$ does not coincide with $\lambda(X_{n,p'})$ for different pairs $(n,p)\neq(n,p')$. However, the*

stretch factors happen to coincide for different pairs occasionally: The kth metallic ratio $\mathfrak{s}_k$ has a formula $(\mathfrak{s}_k)^3 = \mathfrak{s}_{k^3+3k}$ for each $k \in \mathbb{N}$. In particular $(\mathfrak{s}_6)^3 = \mathfrak{s}_{234}$ when $k = 6$. We now claim that $\lambda(X_{n,3}) = \lambda(X_{n,117})$ for all $n = 3^2 2^k$ with $k \geq 5$. Then $117 \leq \lfloor \frac{n}{2} \rfloor$. By Theorem 1.4, we have $\lambda(X_{n,3}) = (\mathfrak{s}_6)^{\frac{2n}{3}} = (\mathfrak{s}_6)^{3\cdot 2^{k+1}}$ and $\lambda(X_{n,117}) = (\mathfrak{s}_{234})^{\frac{2n}{9}} = (\mathfrak{s}_{234})^{2^{k+1}}$. By the equality $(\mathfrak{s}_6)^3 = \mathfrak{s}_{234}$, we have

$$\lambda(X_{n,3}) = ((\mathfrak{s}_6)^3)^{2^{k+1}} = (\mathfrak{s}_{234})^{2^{k+1}} = \lambda(X_{n,117}).$$

5. New numerical periodic solutions of the $2n$-body problem

We numerically found the periodic solutions $\boldsymbol{x}_{n,p}(t)$ for $p = 1, \ldots, \lfloor \frac{n}{2} \rfloor$ in Figure 1. In order to obtain those, we consider the Fourier series of the solutions and compute the Fourier coefficient by using the steepest descent method. Though the existence of the periodic orbits theoretically guarantees for $p = 1, \ldots, \lfloor \frac{n}{2} \rfloor$, new numerical solutions are obtained for several pairs with (n, p) with $\lfloor \frac{n}{2} \rfloor < p < n$. See Figure 12. Then it is natural to ask the following question.

Question 5.1. *For $n \geq 2$ and $\lfloor \frac{n}{2} \rfloor < p < n$, does there exist a periodic solution $\boldsymbol{x}_{n,p}(t)$ of the planar $2n$-body problem whose braid type $X_{n,p}$ is given by the braid $(\beta_{n,p})^{\frac{n}{d}}$ with $d = \gcd(n, p)$?*

If the answer to Question 5.1 is positive, then Theorem 1.4 is extended to some pairs (n, p) with $\lfloor \frac{n}{2} \rfloor < p < n$, i.e. if the answer to Question 5.1 is positive, then the braid type $X_{n,p}$ of the periodic solution $\boldsymbol{x}_{n,p}(t)$ of the planar $2n$-body problem is pseudo-Anosov with the stretch factor $(\mathfrak{s}_{2p})^{\frac{2n}{d}}$. See also Step 1 of the proof of Theorem 1.5.

Acknowledgement

The authors thank the anonymous referee for numerous useful comments.

References

[Bir74] Joan S. Birman. *Braids, links, and mapping class groups*. Princeton University Press, Princeton, N.J.; University of Tokyo Press, Tokyo, 1974. Annals of Mathematics Studies, No. 82.

[Boy94] Philip Boyland. Topological methods in surface dynamics. *Topology Appl.*, 58(3):223–298, 1994.

[Che01] Kuo-Chang Chen. Action-minimizing orbits in the parallelogram four-body problem with equal masses. *Arch. Ration. Mech. Anal.*, 158(4):293–318, 2001.

[Che03] Kuo-Chang Chen. Binary decompositions for planar N-body problems and symmetric periodic solutions. *Arch. Ration. Mech. Anal.*, 170(3):247–276, 2003.

[CM00] Alain Chenciner and Richard Montgomery. A remarkable periodic solution of the three-body problem in the case of equal masses. *Ann. of Math. (2)*, 152(3):881–901, 2000.

[dCH02] André de Carvalho and Toby Hall. The forcing relation for horseshoe braid types. *Experiment. Math.*, 11(2):271–288, 2002.

[FGA21] Marine Fontaine and Carlos García-Azpeitia. Braids of the N-body problem I: cabling a body in a central configuration. *Nonlinearity*, 34(2):822–851, 2021.

[FLP79] A. Fathi, F. Laudenbach, and V. Poenaru. *Travaux de Thurston sur les surfaces*, volume 66 of *Astérisque*. Société Mathématique de France, Paris, 1979. Séminaire Orsay, With an English summary.

[FM12] Benson Farb and Dan Margalit. *A primer on mapping class groups*, volume 49 of *Princeton Mathematical Series*. Princeton University Press, Princeton, NJ, 2012.

[FT04] Davide L. Ferrario and Susanna Terracini. On the existence of collisionless equivariant minimizers for the classical n-body problem. *Invent. Math.*, 155(2):305–362, 2004.

[FT11] Matthew D. Finn and Jean-Luc Thiffeault. Topological optimization of rod-stirring devices. *SIAM Rev.*, 53(4):723–743, 2011.

[Han97] Michael Handel. The forcing partial order on the three times punctured disk. *Ergodic Theory Dynam. Systems*, 17(3):593–610, 1997.

[MM15] Richard Moeckel and Richard Montgomery. Realizing all reduced syzygy sequences in the planar three-body problem. *Nonlinearity*, 28(6):1919–1935, 2015.

[Mona] Richard Montgomery. Some Open Questions in the N-Body Problem (Zoom talk), Sydney Dynamical Group Seminars March 11, 2021.

[Monb] Richard Montgomery. *Four Open Questions in the N-body Problem*. to appear, Cambridge U., Press.

[Mon98] Richard Montgomery. The N-body problem, the braid group, and action-minimizing periodic solutions. *Nonlinearity*, 11(2):363–376, 1998.

[Moo93] Cristopher Moore. Braids in classical dynamics. *Phys. Rev. Lett.*, 70(24):3675–3679, 1993.

[MS13] James Montaldi and Katrina Steckles. Classification of symmetry groups for planar n-body choreographies. *Forum Math. Sigma*, 1:Paper No. e5, 55, 2013.

[Mur74] Kunio Murasugi. *On closed 3-braids*. Memoirs of the American Mathematical Society, No. 151. American Mathematical Society, Providence, R.I., 1974.

[Shi06] Mitsuru Shibayama. Multiple symmetric periodic solutions to the $2n$-body problem with equal masses. *Nonlinearity*, 19(10):2441–2453, 2006.

[Thu88] William P. Thurston. On the geometry and dynamics of diffeomorphisms of surfaces. *Bull. Amer. Math. Soc. (N.S.)*, 19(2):417–431, 1988.

Department of Mathematics, Kyoto University, Yoshida-Honmachi, Sakyo-ku, Kyoto 606-8501, Japan

Email address: kajihara.yuika.6f@kyoto-u.ac.jp

Center for Education in Liberal Arts and Sciences, Osaka University, Toyonaka, Osaka 560-0043, Japan

Email address: kin.eiko.celas@osaka-u.ac.jp

Department of Applied Mathematics and Physics, Graduate School of Informatics, Kyoto University, Yoshida-Honmachi, Sakyo-ku, Kyoto 606-8501, Japan

Email address: shibayama@amp.i.kyoto-u.ac.jp

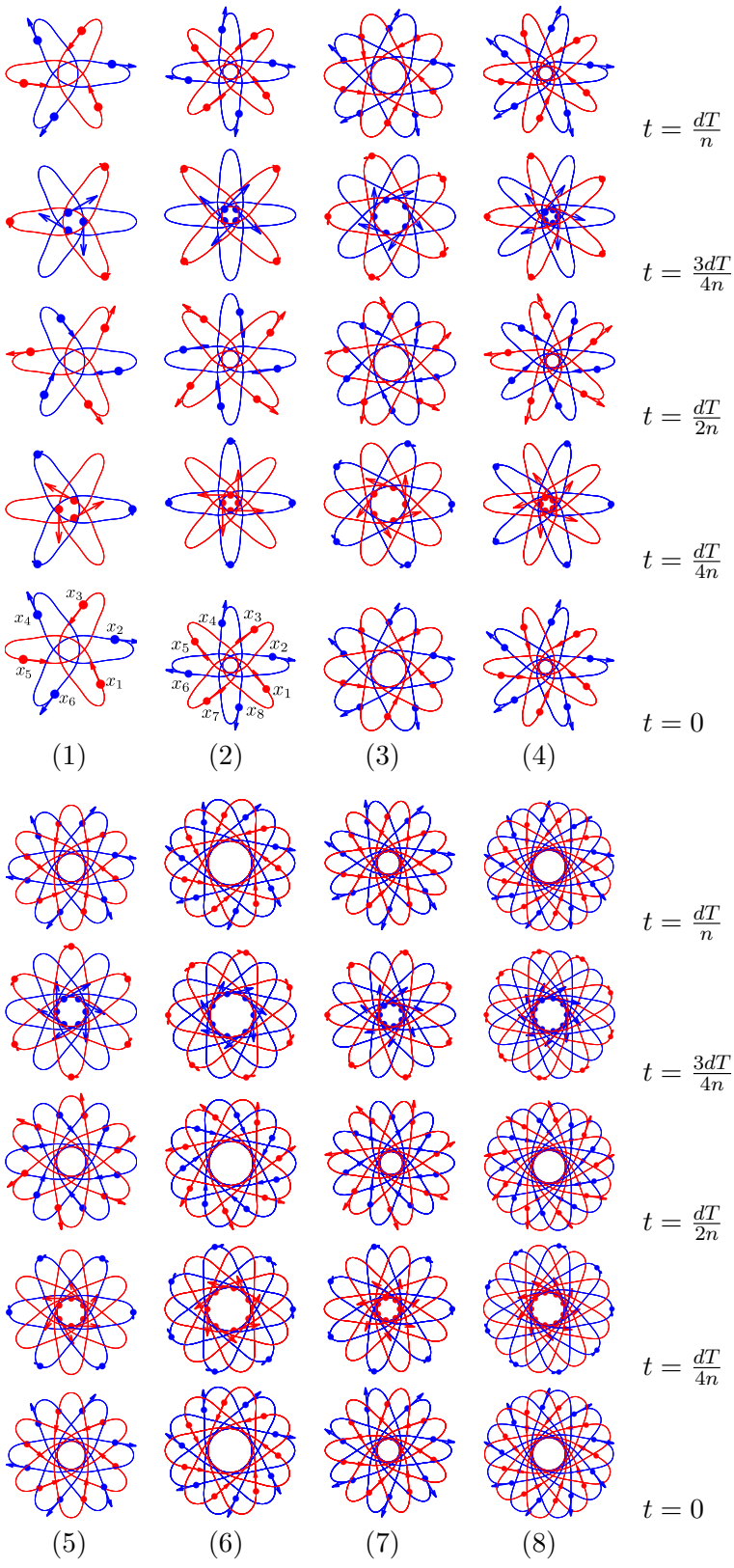

Figure 12. (1) $\boldsymbol{x}_{3,2}(t)$. (2) $\boldsymbol{x}_{4,3}(t)$. (3) $\boldsymbol{x}_{5,3}(t)$. (4) $\boldsymbol{x}_{5,4}(t)$. (5) $\boldsymbol{x}_{6,4}(t)$. (6) $\boldsymbol{x}_{7,4}(t)$. (7) $\boldsymbol{x}_{7,5}(t)$. (8) $\boldsymbol{x}_{9,6}(t)$.